Nanoparticles deposit location control on porous particles in fluidized bed

Laurie Barthe, Karine Philippot, Bruno Chaudret, Nadine Le Bolay, Mehrdji Hemati

NANOPARTICLES DEPOSIT LOCATION CONTROL ON POROUS PARTICLES IN FLUIDIZED BED

Laurie BARTHE[a], Karine PHILIPPOT[b], Bruno CHAUDRET[b], Nadine LE BOLAY[a], Mehrdji HEMATI[a]

[a] *Université de Toulouse - Laboratoire de Génie Chimique – UMR CNRS 5503 – INP-ENSIACET 5 rue Paulin Talabot, BP 1301, 31106 Toulouse cedex 01 – France*
[b] *Laboratoire de Chimie de Coordination – UPR CNRS 8241, 205 route de Narbonne, 31077 Toulouse cedex 04 – France*

Abstract: The nanoparticles synthesis and deposition can be carried out using an innovating technique named dry impregnation in a fluidized bed. Its principle consists in the spraying of a solution containing a metallic precursor or preformed nanoparticles into a hot fluidized bed of porous particles.

The solvent vapour saturation rate value, τ_s, defined as the ratio between the solvent content in the bed atmosphere and the maximum solvent content, appears as a key parameter allowing predicting the deposit location.

Three operation conditions can be distinguished:

- "Unstable conditions" for high τ_s (between 1 and 0.8). The operation is unstable: a low increase of the liquid flow rate, or a reduction of the gas inlet temperature, can lead to wet quenching.
- "Operating conditions" or "slow drying conditions" for intermediate values of τ_s (between 0.8 and 0.2).
- "Fast drying conditions" characterized by high bed temperatures and low solvent saturation rates ($\tau_s < 0.2$).

This paper presents experimental results obtained during the dry impregnation of coarse and fine porous particles using different types of precursors: inorganic precursors (metallic salts), metal organic complexes and a colloidal suspension containing preformed metallic nanoparticles (rhodium). The operating conditions were chosen in order to study the three operation conditions previously described.

Interesting results were obtained concerning the deposit distribution within the support grains at the local scale, Indeed, it appeared that a fast drying leads to a deposit located only at the external particle surface (like coating), whereas a uniform deposit on the whole particle volume is obtained with slow drying conditions.

Keywords: metallic nanoparticles, fluidized bed, dry impregnation, solvent vapour saturation rate, deposit location, porous support.

1. INTRODUCTION

Usually, the preparation method of composite materials such as supported catalysts consists in the immersion of the chosen support in a precursor solution under stirring to favour the diffusion inside the support grains. After this impregnation, the composite material successively undergoes the stages of filtration, drying and calcination/activation. This technique is easy to carry out but presents a weakness: the dependence of the deposit location on the physico-chemical properties of the solution-support couple. Indeed, a control of the deposit location represents a real challenge, particularly in catalysis (Fulton, 1986; Lekhal *et al.*, 2001). Moreover, to obtain a high metal loading, these four steps should be repeated several times.

Supported catalysts synthesis can also be achieved using another innovating technique, namely dry impregnation in a fluidized bed (Barthe *et al*,. 2007b). This technique is a “one pot process”. It consists in spraying a precursor solution into a hot fluidized bed of porous particles. The penetration of each drop of the metallic solution in the porous solid particles and the solvent evaporation take place at the same time. The efficiency of the metal deposition is close to 100 % and the metal loading is directly related to the operating time and the liquid flow rate and concentration. It is found that a competition between the two phenomena, drying and capillary suction, controls the deposit location.

In order to determine the importance of the solvent evaporation process compared to the solution penetration by capillarity, an impregnation module, IM, was defined. It is the ratio between the drying characteristic time (t_{dry}) and a capillary penetration time (t_{cap}).

- t_{cap}, the necessary time for liquid penetration in the pores, can be estimated from the following equation taken from the model of the parallel capillary beam (Burdine, 1953):

$$t_{cap} = \frac{2\mu x^2}{\gamma_{LV} \cos\theta r_{pore}} \quad (1)$$

where μ is the liquid viscosity, x the pore length equivalent to the radius particle multiplied by the tortuosity factor, γ_{LV} the interfacial tension, θ the contact angle and r_{pore} the pore radius.

- t_{dry} is the time necessary for a particle saturated by pure solvent to be transformed into a dry particle under defined fluidized bed conditions (temperature and humidity). The calculation of this characteristic time is based on the mass and energy balances on a single wet particle considering that the mass transfer is controlled by external resistance (gas phase). The model's equations described in previous works (Desportes, 2005; Barthe *et al.*, 2007b) leads to the following equation:

$$t_{dry} = \frac{d_p \chi \rho_s}{6k_y (Y_i - \bar{Y})} \quad (2)$$

where d_p is the particle diameter, χ the internal support porosity, ρ_s the solvent density, k_y the overall mass transfer coefficient, $\bar{Y}$ the average solvent content in the bed atmosphere determined by overall mass balance on the reactor, and Y_i the absolute solvent content at the interface (depending on the particle temperature and humidity).

Moreover, another criterion was considered to determine the deposit location: τ_s, the solvent vapour saturation rate value. It is defined as the ratio between solvent content in the bed atmosphere and the maximum solvent content. It should be noted that τ_s depends on $\bar{Y}$ and bed temperature.

In conclusion, the adequate choice of the operating conditions (bed temperature, liquid and fluidization gas flow rate) based on the two key parameters, τ_s and IM, allows controlling the deposit location.

- For high τ_s ($0.8 \leq \tau_s \leq 1$) and high IM, the operation is unstable and wet quenching is observed.
- For slow drying conditions ($0.2 \leq \tau_s \leq 0.8$ and IM greater than 10), the metallic precursor deposit is located inside the porous matrix.
- For fast drying conditions ($\tau_s < 0.2$ and IM less than 10), the deposit is located on the support particle surface.

This study gathers experiments carried out to prepare composite materials, using various types of precursors (metallic salts, metal organic precursors solutions and colloidal suspensions containing preformed metal nanoparticles) and various particle sizes (from 100 µm to a few millimetres). This work aims to show that τ_s is a key parameter, and when coupled with IM, it permits to control the deposit location. With an appropriate choice of the operating conditions, it is possible to adjust the τ_s value, and consequently IM thus governs the deposit location.

II. METHODS AND MATERIALS

2.1 Supports and metal sources

Two solids, different in their nature and grains size, were used as catalysts supports: fine porous silica particles and coarse activated γ alumina particles. Their principal physical properties are reported in Table 1.

Table 1 Physical properties of the porous supports

Properties	Silica gel	Alumina
Mean diameter d_p (µm)	120	2 400
Specific surfaces S_{bet} (m^2/g)	530	330
Pore volume V_p (cm^3/g)	0.8	0.3

Various types of precursors were sprayed on the supports: metallic salts (Iron nitrate and Manganese nitrate), metal organic precursors solutions (Palladium allyl chloride) and colloidal suspensions containing preformed metal nanoparticles (Rhodium suspension).

2.2 Experimental set-up

Depending on the metal source nature, the experiments were carried out under air or controlled atmosphere (inert or reductive) in a batch fluidized bed. This reactor is a stainless steal cylindrical column with 0.1 m inner diameter and 0.5 m in height, described by Barthe (2007a).
The gas distributor is a stainless steel perforated plate with a porosity of 0.5 %. The fluidizing gas flow rate is measured by means of a rotameter and preheated by an electrical heater before entering the bed. The elutriated particles and solvent vapours are collected at the column outlet respectively by a cyclone and a condenser.
The metallic precursor solution is drawn up by a volumetric pump from a reservoir to an internal mixing two–fluid spray nozzle. The atomizing gas flow rate is controlled by a needle valve and measured by a rotameter. The bed temperature is controlled by means of a PID regulator. Monitoring of temperature and pressure drop takes place during operation.
The solid sampling system is achieved with a vacuum circuit. The sampling with a controlled atmosphere is done through a nitrogen circuit. In addition it enables working with oxygen and water sensitive products.

2.3 Characterization methods

The metal deposit location of the samples was studied using different techniques. The composite materials were analysed by an optical microscope and a Transmission Electron Microscope (TEM). In case of TEM observations, the samples were cut by ultramicrotomy.

2.4 Operating conditions

The different operating conditions are listed in Table 2. The first six experiments were carried out with inorganic precursors. Organometallic complexes have been used in experiment 7 while for experiments 8 and 9 a colloidal suspension was sprayed. For each precursor type various experiments were carried out corresponding to different values of IM and τ_s (and to the three zones previously defined).
The pure solvent used is water except for experiment 7 for which tetrahydrofuran (THF) was used since the corresponding precursor is water sensitive.

Table 2 Experimental conditions

Experiment number	S1	S2	S3	S4	S5	S6	S7	S8	S9
Precursor name	Iron nitrate				Manganese nitrate		Palladium allyl chloride	Rhodium suspension	
Support	Silica gel				γ Alumina		Silica gel	Silica gel	
Solvent nature	water				water		THF	water	
Gas flow rate (m^3/h)	0.8	0.8	0.8	0.8	31	28	0.8	0.8	0.8
Fluidized bed temperature (°C)	46	64	86	136	27	45	25	45	106
IM (-)	380	80	40	20	20	4	21	400	28
Solvent vapour saturation rate τ_s (-)	0.78	0.34	0.14	0.01	0.70	0.08	0.11	0.77	0.01

The operating conditions choice to obtain various deposit location of the precursor in the support can be done very easily. The experiments should be carried out keeping the same solution and fluidisation gas flow rate, modifying only the bed temperature. It is the case of the experiments S1 to S4 (for iron deposit) and experiments S8 and S9 (for rhodium deposit). Then, it is possible to plot the evolution of the two parameters τ_s and IM according to the bed temperature (Figure 1 a and b). The graph can be divided into the three zones previously described: unstable (1), slow drying (2) and fast drying (3).
According to the operating conditions and to the values of τ_s and IM, the experiments S1 to S4 can be plotted on the graph of Figure 1a. It is possible to confirm the operation conditions and predict the deposit location through the choice of the bed temperature. The same can be done with the experiments S8 and S9 (Figure 1b).

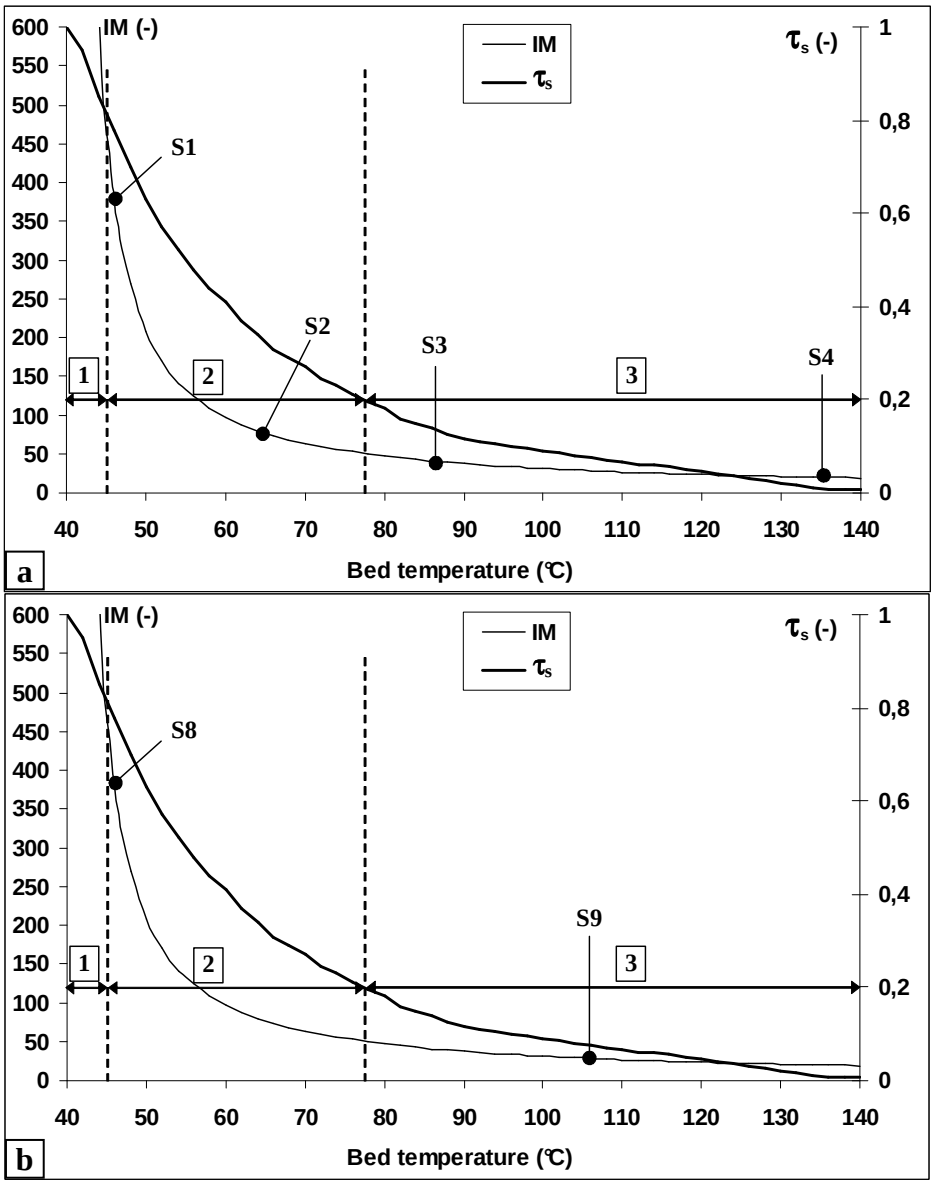

Fig. 1. IM and τ_s evolution with the bed temperature (a: Iron deposit - b: Rhodium deposit)

III. RESULTS AND DISCUSSION

The deposit location of Palladium-, Iron- and Manganese- composite materials was studied after an activation step leading to the formation of metallic nanoparticles. In the case of organometallic precursors (Palladium) the activation step is operated under a nitrogen/hydrogen mixture at 80 °C during 90 minutes, while for inorganic precursors the samples are heated up in air to 450 °C (for Iron) or to 300 °C (for Manganese). Activation and calcination conditions were chosen to favor the formation of easily observable metallic nanoparticles clusters. These conditions were not optimized to obtain small individual nanoparticles (Barthe *et al.*, 2008b). In case of rhodium composite materials, the deposit is already formed by metallic nanoparticles.

3.1 Unstable conditions

A few experiments were carried out in "unstable conditions" ($\tau_s > 0.8$) in the case of iron nitrate spraying on fine porous silica particles. It was verified that those experiments could not be completed due to wet quenching.

3.2 Slow drying conditions

Some of the experiments were carried out under operating conditions corresponding to slow drying ($0.2 \leq \tau_s \leq 0.8$ and high IM) using inorganic precursors (S1, S2 and S5) and a colloidal suspension (S8).
The samples S1 and S8 were analysed by TEM (Figure 2 a and b).

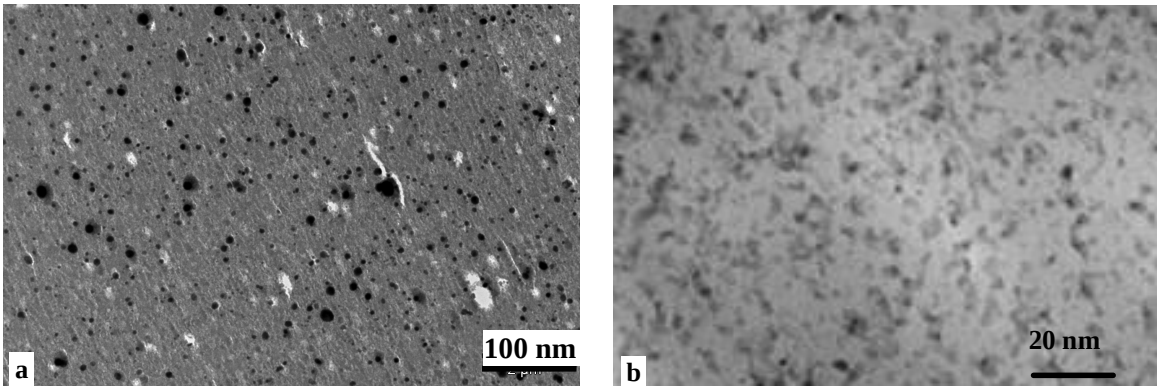

Fig. 2. TEM micrographs of various metallic nanoparticles on silica a) Iron (S1) b) Rhodium (S8)

The micrographs shows that the deposit, characterized by the most darkened zones, is quasi uniform in the entire particle volume in case of Iron nanoparticles (a) and Rhodium nanoparticles (b). In slow drying conditions, whatever the precursor nature, dry impregnation on fine porous particles leads to homogenous deposit.

Thus, experiment S5 was carried out with coarse alumina particles, to verify if this result, obtained with fine particles, is similar with bigger particles. The sample was prepared by spraying an inorganic precursor on coarse alumina particles. Three samples were removed from the fluidized bed at different operation times to characterize the evolution of the deposit distribution during the impregnation. They are numbered from 1 to 3, in the ascending order of time residence in the bed and so of the metal deposit quantity. The cross section photographs are presented in Figure 3.

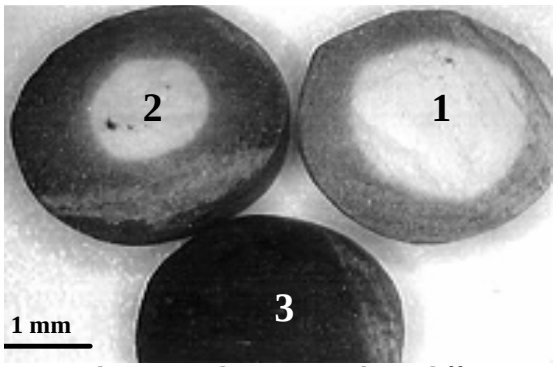

Fig. 3. Microscope micrographs of Manganese deposit on alumina particles at different operating times (S5)
1 corresponds to 30 minutes, 2 to 90 minutes and 3 to 170 minutes

These images show that the aqueous solution penetrates into the alumina particles. Moreover, the precursor deposit inside the solid is similar to the displacement of a front from the particle periphery towards its centre (Samples 1 to 3). This internal position of the impregnation front is a function of the impregnation rate. For samples 1 and 2, the precursor is rather on the particle borders (egg shell catalysts). For sample S3, the precursor reached the particle centre. The deposit is then uniform in the whole particle volume.
This phenomenon is comparable to a heterogeneous reaction between a gas and a porous solid when the diffusion penetration time of the reactive gas is very high compared to the chemical reaction time. In this case, the reaction proceeds following a shrinking core model developed in a previous article (Barthe *et al.*, 2008a).

3.3 Fast drying conditions

Other experiments were carried out under fast drying conditions (τ_s < 0.2 and low IM) using inorganic precursors (S3, S4 and S6), an organometallic precursor (S7) and a colloidal suspension (S9).
Samples obtained for experiments S4, S7 and S9 were analysed by TEM (Figure 4 a, b and c). For each micrograph a deposit at the particle surface is observed, like a surface coating. The thickness of this coat can be controlled by the precursor quantity (and thus by the operation time) and is composed of individual nanoparticles into clusters. In fast drying conditions, whatever the precursor nature is, the deposit is located at the silca particles surface.

To verify again that the conclusion obtained with fine particles can be extended to coarse particles, experiment 6 was carried out. S6 was analysed by microscopy. For fast drying conditions, micrographs of the external surface and the cross section of the samples presented in Figure 4 d reveal that the deposit is located at the particle surface, with the intermediate and central zones remaining virgin.

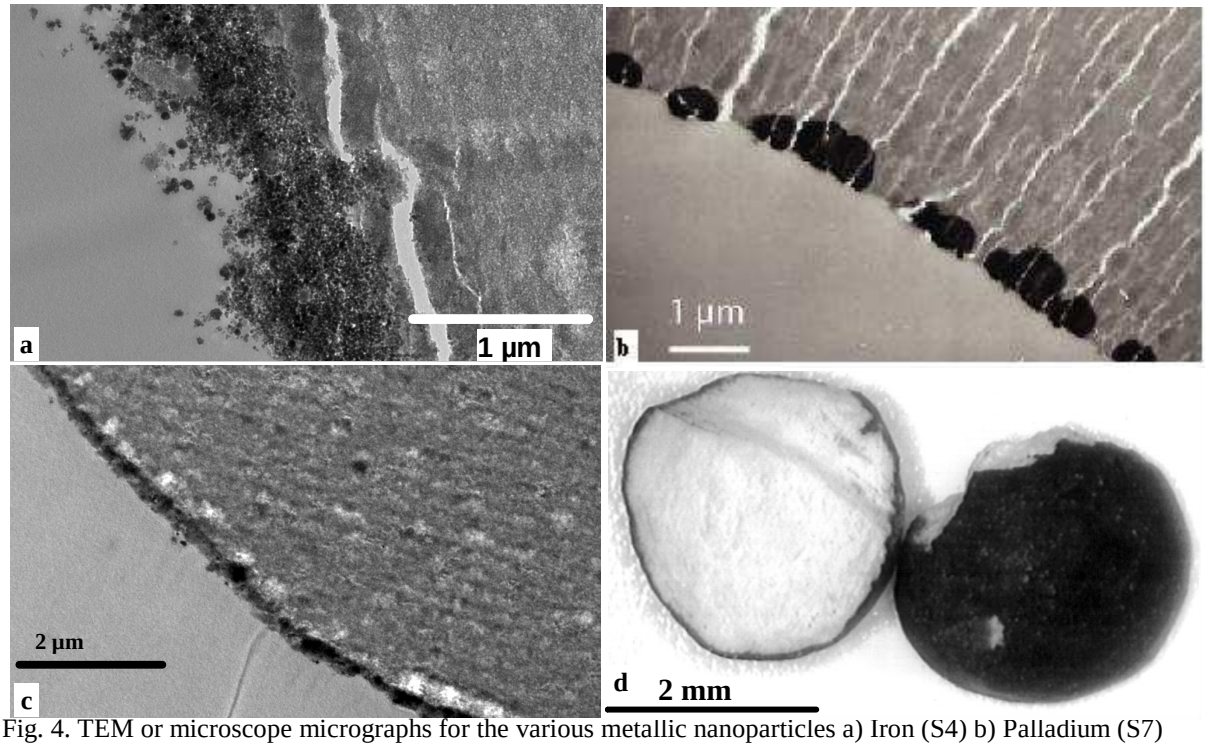

Fig. 4. TEM or microscope micrographs for the various metallic nanoparticles a) Iron (S4) b) Palladium (S7) c) Rhodium (S9) and d) Manganese (S6)

IV. CONCLUSION

A key parameter allowing the prediction of the deposit location was identified: τ_s, the solvent vapour saturation rate, defined as the ratio between the solvent content in the bed atmosphere and the maximum solvent content. Three operation conditions can be distinguished:

- "Unstable conditions" are observed for high τ_s ($0.8 \leq \tau_s \leq 1$) and are characterized by a fast decrease of IM. The operation is unstable: a low increase of the liquid flow rate or a reduction of the gas inlet temperature can lead to wet quenching. The deposit is not possible.
- "Slow drying conditions" are characterized by intermediate values of τ_s ($0.2 \leq \tau_s \leq 0.8$) and IM greater than 10. The solid precursor deposit takes place homogeneously inside the particles homogeneously.
- "Fast drying conditions" are characterized by high bed temperatures and low solvent saturation rates ($\tau_s < 0.2$). The deposit is then located on the particle external surface (egg shell catalysts).

Moreover, all results show that the deposit location can be controlled during the dry impregnation process whatever the precursor nature (organic, inorganic or colloidal suspension) and for a large range of support particle sizes (from 100 µm to few millimetres).

REFERENCES

Barthe, L, (2007a), Synthèse et dépôt de nanoparticules métalliques dans un support poreux par imprégnation en voie sèche dans un lit fluidisé : élaboration de catalyseurs supportés, *PhD thesis, INP Toulouse*

Barthe, L., S. Desportes, M. Hemati, K. Philippot and B. Chaudret, (2007b). Synthesis of supported catalysts by dry impregnation in fluidized bed. *Chem Eng Res and Des*, 85(A6), 1–11

Barthe, L., S. Desportes, D. Steinmetz and M. Hemati, (2008a). Metallic salt deposition on porous particles by dry impregnation in fluidized bed: Effect of drying conditions on metallic nanoparticles distribution. *Chem Eng Res Des* doi:10.1016/j.cherd.2008.07.002

Barthe, L., M. Hemati, K. Philippot and B. Chaudret, (2008b) Dry impregnation in fluidized bed: Drying and calcination effect on nanoparticles dispersion and location in a porous support *Chem Eng Res and Des*, 86(4), 349–358

Burdine, N. T., (1953). Relative permeability calculations from pore size distribution data, *Petroleum Trans. Am. Inst. Mining Eng.*, 198, 71–77

Desportes, S., (2005). Imprégnation en voie sèche en lit fluidisé, application à la synthèse de catalyseurs supportés, PhD thesis, INP Toulouse

Fulton, J.W., (1986). Selecting the catalyst configuration, *Chem. Eng.*, 93, 97–101

Lekhal, A., B. Glasser and J.G. Khinast, (2001). Impact of Drying on Catalyst Profile of supported Impregnation Catalysts, *Chem Eng. Sci.*, 56 (15), 4473–4487